© 2014. Published by The Company of Biologists Ltd | Journal of Cell Science (2014) 127, 2471–2482 doi:10.1242/jcs.139626

RESEARCH ARTICLE

IPS-1 plays an essential role in dsRNA-induced stress granule formation by interacting with PKR and promoting its activation

Peifen Zhang[1,2,*], Yuye Li[1,2,*], Jun Xia[1,2], Junfang He[1,2], Jieying Pu[1,2], Jiong Xie[1,2], Siyu Wu[1,2], Lianqiang Feng[1,2], Xi Huang[1,2] and Ping Zhang[1,2,‡]

ABSTRACT

The formation of cytoplasmic stress granules and the innate immune response are two distinct cellular stress responses. Our study investigated the involvement of four innate immune proteins – retinoic-acid-inducible gene I (RIG-I, also known as DDX58), melanoma differentiation-associated gene 5 (MDA5, also known as IFIH1), IFN-β promoter stimulator (IPS-1, also known as MAVS) and protein kinase regulated by dsRNA (PKR, also known as EIF2AK2) in the formation of stress granules. Knockdown of IPS-1 or PKR significantly decreased the formation of stress granules induced by double-stranded (ds)RNA. IPS-1 depletion markedly attenuated the phosphorylation of PKR and eIF2α that was triggered by dsRNA, and IPS-1 facilitated the *in vitro* autophosphorylation of PKR. In IPS-1-depleted cells, the dsRNA-mediated dimerization of PKR through its dsRNA-binding domains was significantly abrogated, suggesting that IPS-1 might be involved in PKR dimerization. By co-immunoprecipitation and pulldown assays, our data demonstrate that IPS-1 directly binds to PKR through the IPS-1 caspase activation and recruitment domain (CARD), suggesting that the effect of IPS-1 on the formation of stress granules might be exerted through interacting with PKR and mediating its activation. PKR was recruited into stress granules upon activation, whereas the majority of IPS-1 protein formed clusters on mitochondrial membranes. Our work provides the first evidence that the innate signaling molecule IPS-1 plays an essential role in stress granule formation.

KEY WORDS: Stress granule, IPS-1, PKR, dsRNA

INTRODUCTION

Eukaryotic cells form macromolecular aggregates called stress granules in response to different stress conditions, such as heat shock, oxidative stress, endoplasmic reticulum (ER) stress, UV irradiation and viral infections (Kedersha and Anderson, 2002). Stress granule formation might initiate from the phosphorylation of eukaryotic translation initiation factor 2α (eIF2α) by four kinases – protein kinase regulated by dsRNA (PKR, also known as EIF2AK2), heme-regulated kinase (HRI, also known as EIF2AK1), general control nondepressible 2 kinase (GCN2, also known as EIF2AK4) and PKR-like ER kinase (PERK, also known as EIF2AK3) (Anderson and Kedersha, 2002). In some circumstances, stress granule formation might occur independently of eIF2α phosphorylation, such as during hippuristanol-induced stress (Anderson and Kedersha, 2008; Grousl et al., 2013; Mazroui et al., 2006; Qin et al., 2011).

The components of stress granules include stalled 48S initiation translation complexes and a group of RNA-binding proteins, such as T-cell-restricted intracellular antigen-1 (TIA-1), TIA-1-related protein (TIAR, also known as TIAL1) and Ras GAP SH3-domain-binding protein 1 (G3BP-1) (Anderson and Kedersha, 2008; Ohn and Anderson, 2010). In addition, other cellular proteins could be packed into stress granules, including Tudor Staphylococcal Nuclease (Tudor-SN, also known as SND1), adenosine deaminase acting on RNA 1 (ADAR1) (Weissbach and Scadden, 2012), DAZL (Kim et al., 2012), p90 ribosomal S6 kinase 2 (RSK2, also known as RPS6KA3), Ras homolog gene family member A and Rho-associated coiled-coil forming kinase 1 (RhoA and ROCK1) (Tsai and Wei, 2010), 2-oxoglutarate and Fe(II)-dependent oxygenase domain containing 1 (OGFOD1) (Wehner et al., 2010), melanoma differentiation-associated gene 5 (MDA5, also known as IFIH1) and retinoic-acid-inducible gene I (RIG-I, also known as DDX58) (Langereis et al., 2013; Onomoto et al., 2012). When conditions that are suitable for translation are restored, the components of stress granules are dynamically released so that translation is rapidly resumed. Therefore, stress granules are believed to serve as a temporary repository for translationally silent mRNA, thereby promoting cellular survival (Anderson and Kedersha, 2002; Arimoto et al., 2008; Tsai and Wei, 2010).

Innate immunity is another cellular response against external stress, particularly that induced by microbial invasion (Takeuchi and Akira, 2010). During viral infection, double-stranded (ds)RNA, a viral replication intermediate (Alexopoulou et al., 2001), is detected as a pathogen-associated molecular pattern (PAMP) by cellular receptors, including membrane-bound Toll-like receptor 3 (TLR3) (Akira and Takeda, 2004), cytoplasmic RIG-I and MDA5 (Kang et al., 2002; Yoneyama et al., 2004). RIG-I and MDA5 act as sensors that detect intracellular viral dsRNA, and they initiate signaling through IFN-β promoter stimulator (IPS-1, also known as Cardif, MAVS or VISA), which is expressed on the mitochondrial membrane (Kawai et al., 2005). Upon binding to RIG-I or MDA5, IPS-1 undergoes a conformational change, switching to prion-like aggregates and transmitting the innate signaling through the TBK-1 and IKK kinases, thus leading to the induction of proinflammatory cytokines and IFNs (Hou et al., 2011; Meylan et al., 2006; Seth et al., 2005). Recent studies have shown that several

[1]Department of Immunology, Institute of Human Virology, Zhongshan School of Medicine, Sun Yat-sen University, Guangzhou 510080, China. [2]Key Laboratory of Tropical Diseases Control (Sun Yat-sen University), Ministry of Education, Guangzhou 510080, China.
*These authors contributed equally to this work

‡Author for correspondence (zhangp36@mail.sysu.edu.cn)

Received 30 July 2013; Accepted 12 March 2014

Journal of Cell Science

Journal of Cell Science (2014) 127, 2471–2482 doi:10.1242/jcs.139626

RNA-binding proteins involved in innate immune signaling, including RIG-I, MDA5, PKR and ADAR1, are packed into influenza A virus (IAV)-induced antiviral stress granules (avSGs) (Onomoto et al., 2012) and mengovirus- and measles-virus-induced stress granules (Langereis et al., 2013; Okonski and Samuel, 2013). Nevertheless, it is unclear whether these proteins have a direct impact on stress granule formation.

The aim of the current study was to examine the relationship between stress granule formation and the innate immune response. We investigated the role of four key molecules associated with innate immunity (the intracellular sensors PKR, RIG-I and MDA5, and the adaptor IPS-1) in stress granule formation induced by different stresses. We found that IPS-1 and PKR play a crucial role in the process of stress granule formation induced by dsRNA, a common viral byproduct, but not by other stresses. We found that IPS-1 is physically associated with PKR and promotes PKR activation. For the first time, we demonstrate an unexpected role for IPS-1 in mediating stress granule formation, which it performs in addition to its well-defined role in innate immunity.

RESULTS

IPS-1 and PKR play an essential role in dsRNA-induced stress granule formation

To examine whether innate immune proteins, including the dsRNA sensors RIG-I, MDA5, PKR and an adaptor protein IPS-1, have a direct impact on the formation of stress granules, we silenced these proteins by RNAi and compared the extent of stress granule formation induced by two eIF2α-dependent stimuli (dsRNA and heat shock) and one eIF2α-independent stimulus (hippuristanol). The efficacy of each siRNA was monitored by western blotting or real-time PCR. Western blotting data showed that >95% of RIG-I, IPS-1 and PKR protein was depleted in cells transfected with the respective siRNA, validating a high efficacy of siRNA-mediated knockdown (Fig. 1A–C). To assess the extent of MDA5 knockdown, we measured its mRNA level instead of the protein level, owing to its low endogenous abundance in A549 cells (Fig. 1D).

Subsequently, these siRNA-transfected cells were mock-treated or stimulated with the immunostimulant polyinosinic:polycytidylic acid [poly(I:C)], a synthetic analog of dsRNA. The high molecular mass (hereafter referred to as high molecular weight, HMW) version of poly(I:C) is sensed by MDA5, whereas the low molecular mass (low molecular weight, LMW) version is sensed by RIG-I. The percentages of stress-granule-positive cells were determined in an immunofluorescence staining assay using an antibody against TIA-1, a classical hallmark of stress granules (Anderson and Kedersha, 2002). In HMW-poly(I:C)-transfected cells, knockdown of PKR significantly reduced the percentage of TIA-1-positive cells (Fig. 1E,F). Interestingly, the formation of stress granules was also significantly reduced in IPS-1-depleted cells (22% contained stress granules, versus 42% of cells treated with a control siRNA, $P<0.001$). The knockdown of MDA5 led to a smaller but still significant effect on stress granule formation ($P<0.05$). By contrast, the percentage of stress-granule-positive cells was comparable between RIG-I-knockdown and control cells ($P>0.05$). Moreover, the depletion of both RIG-I and MDA5 also led to a significant reduction in the amount of stress granule formation ($P<0.01$). Similarly, in LMW-poly(I:C)-transfected cells (Fig. 1G,H), a significant reduction in the percentage of stress-granule-positive cells was seen in cells that were depleted of PKR, IPS-1, MDA5 or RIG-I and MDA5, but not in cells that were depleted of RIG-I alone (Fig. 1G,H). Moreover, the formation of stress granules in response to heat shock and hippuristanol treatment was examined. Both heat shock and hippuristanol treatment led to stress granule formation in most cells (70% and 98% of cells, respectively). However, the depletion of none of the innate immune molecules had any significant effect on stress granule formation in response to heat shock or hippuristanol (Fig. 1I–K). These data suggested that role of PKR and IPS-1 in the formation of stress granules was dsRNA specific, but was independent of dsRNA length.

IPS-1 affects stress granule formation by regulating the phosphorylation of PKR and eIF2α

As PKR–eIF2α is the dominant signaling pathway involved in dsRNA- and virus-induced formation of stress granules, we hypothesized that the effects of IPS-1 and MDA5 on stress granule formation might be exerted through PKR and eIF2α. To test this hypothesis, we compared the activation levels of PKR and eIF2α in cells depleted of RIG-I, MDA5, IPS-1 or PKR. Cells were stimulated by treatment with poly(I:C), and the phosphorylated (active) forms of PKR and eIF2α were detected by western blotting with specific antibodies. In HMW-poly(I:C)-treated cells, phosphorylation of PKR and eIF2α was detected more readily than in control cells, as expected (Fig. 2A, lane 2 versus lane 1). Interestingly, the phosphorylated forms of PKR and eIF2α were dramatically reduced in IPS-1- or PKR-knockdown cells upon poly(I:C) transfection (Fig. 2A, lanes 4 and 10 versus lane 2), suggesting that IPS-1 influences PKR activation. MDA5 depletion impaired the phosphorylation of PKR and eIF2α to a more moderate extent (lane 8), whereas knockdown of RIG-I did not affect phosphorylation of PKR and eIF2α in response to poly(I:C) (lane 6 versus lane 2). Likewise, knockdown of IPS-1 and PKR, but not of RIG-I, significantly reduced the activation of PKR and eIF2α in LMW-poly(I:C)-treated cells (Fig. 2B). However, MDA5 deficiency did not decrease the amount of phosphorylated PKR and eIF2α in response to treatment with LMW poly(I:C) (lane 6 versus lane 2), which might be due to the lack of responsiveness of MDA5 to short-length dsRNA. To further examine the redundancy of RIG-I and MDA5 in dsRNA sensing and stress granule formation, cells were simultaneously transfected with siRIG-I and siMDA5, followed by challenge with HMW and LMW poly(I:C). Western blotting data showed that the PKR activation triggered by HMW poly(I:C), but not by LMW- poly(I:C), was reduced in cells depleted of both RIG-I and MDA5, as seen in MDA5-depleted cells (Fig. 2C,D), suggesting that MDA5 but not RIG-I was involved in the formation of stress granules. Of note, the total PKR protein amounts in all poly(I:C)-treated cells were lower than in control cells, which is most likely caused by translational inhibition or a caspase-dependent cleavage of PKR protein (Saelens et al., 2001), consistent with our previous observations (Zhang and Samuel, 2007). Total protein levels of eIF2α were comparable in each lane.

To further validate the role of IPS-1in PKR autophosphorylation, purified IPS-1 and PKR proteins were used in a PKR kinase assay. The reaction mixtures were subjected to western blotting using the monoclonal antibody against phospho-PKR (Thr446). As shown in Fig. 2E, the IPS-1 protein alone clearly increased the phosphorylation of PKR on Thr446 (lane 3) and further enhanced PKR phosphorylation in the presence of poly(I:C) (lane 4). Surprisingly, poly(I:C) alone did not induce the phosphorylation of PKR on Thr446 (lane 2). These data

Journal of Cell Science (2014) 127, 2471–2482 doi:10.1242/jcs.139626

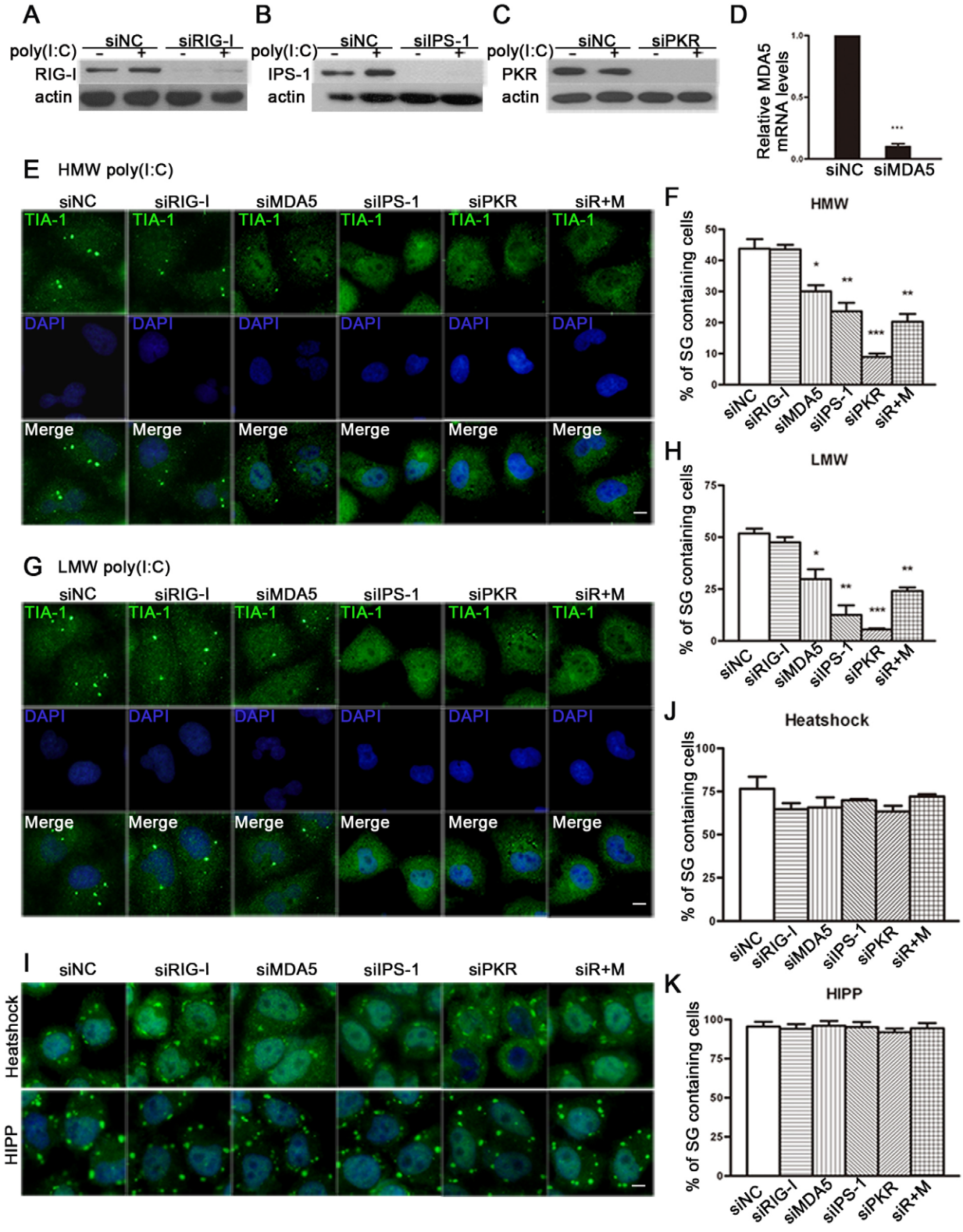

Fig. 1. IPS-1 and PKR play an essential role in poly(I:C)-induced stress granule formation. A549 cells were transfected with siNC, siRIG-I, siMDA5, siIPS-1, siPKR or a combination of siRIG-I and siMDA5 (siR+M), and were then stimulated with poly(I:C), heat shock or hippuristanol (HIPP), or left untreated. (A–C) RIG-I, IPS-1 and PKR protein levels in siRNA-transfected cells were determined by western blotting. (D) MDA5 mRNA level was measured by real-time PCR. (E–K) Immunofluorescence microscopy images and quantification of the percentage of cells containing stress granules under conditions of HMW poly(I:C) stimulation (E,F), LMW poly(I:C) stimulation (G,H) or heat shock or hippuristanol stimulation (I,J,K). Cells were stained for TIA-1 (green) and nuclei were visualized with DAPI (blue). PicCnt 100× was used to determine the percentages of cells containing stress granules. Data are shown as the mean±s.e.m. (≥200 cells from each culture in three independent experiments); *$P<0.05$, **$P<0.01$, ***$P<0.001$. Scale bars: 10 μm.

Journal of Cell Science (2014) 127, 2471–2482 doi:10.1242/jcs.139626

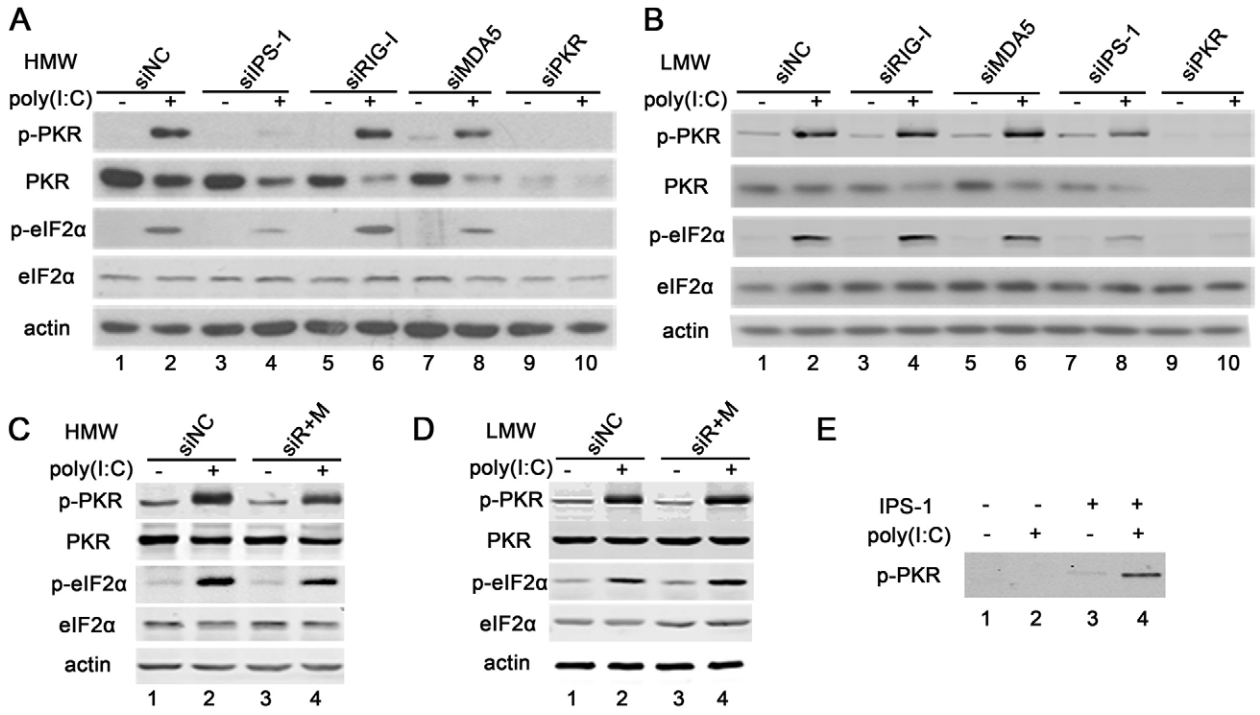

Fig. 2. IPS-1 stimulates the phosphorylation of PKR. A549 cells were transfected with siNC, siIPS-1, siRIG-I, siMDA5 or siPKR, and then mock-transfected or transfected with HMW (A) or LMW (B) poly(I:C). Alternatively, cells were transfected with siNC or a combination of siRIG-I and siMDA5, followed by stimulation with HMW (C) or LMW (D) poly(I:C). Cells were harvested for western blotting to detect the phosphorylated forms (p) and total protein levels of PKR and eIF2α. β-actin was used as an internal loading control. (E) PKR kinase assay. Purified IPS-1 and PKR proteins were incubated in kinase reaction mixture for 30 min. Reaction mixtures were then used for SDS-PAGE and western blotting to detect PKR phosphorylation on Thr446. Data are representative of at least three independent experiments.

suggested that the PKR autophosphorylation on Thr446 was dependent on IPS-1.

IPS-1 knockdown abolishes the association of PKR with its dsRNA-binding domains or full-length PKR

The activation of PKR involves binding to dsRNA, dsRNA-binding domain (dsRBD)-mediated dimerization and autophosphorylation (Lemaire et al., 2006; Sadler, 2010). To address the mechanism by which IPS-1 facilitates PKR activation, we examined the involvement of IPS-1 in PKR dimerization through co-immunoprecipitation (co-IP) assays. First, as the PKR N-terminus has been suggested to mediate PKR dimerization (Patel and Sen, 1998), we overexpressed an HA-tagged version of the PKR N-terminus (PKRN–HA) comprising two dsRBDs in IPS-1-sufficient or IPS-1-deficient cells, followed by poly(I:C) stimulation (to mimic exposure to dsRNA). Protein was pulled down from whole-cell extracts using an anti-HA antibody, and protein complexes were detected by western blotting using an anti-PKR antibody. The endogenous full-length PKR was precipitated with PKRN–HA regardless of the absence or presence of dsRNA (Fig. 3A, upper panel, lanes 1–4). Upon stimulation with dsRNA, more endogenous co-immunoprecipitated PKR was detected in control (siNC)-transfected cells (upper panel, lane 2 versus lane 1), and this dsRNA-mediated association between PKR and PKRN–HA was significantly reduced in IPS-1-depleted cells (upper panel, lane 4 versus lane 3).

Next, we generated a construct expressing full-length PKR tagged with HA at the N-terminus and FLAG at the C-terminus (HPKRF) to further probe the role of IPS-1 in PKR activation. IPS-1-sufficient or IPS-1-deficient cells were transfected with pSG5-HPKRF plasmid and harvested for co-IP using an anti-FLAG antibody. Without dsRNA stimulation (Fig. 3B), comparable amounts of endogenous PKR (lower band) were precipitated with HPKRF (upper band) in IPS-1-sufficient and IPS-1-deficient cells (lanes 1 and 3). Stimulation with dsRNA significantly increased the PKR–HPKRF association (upper panel, lane 2 versus lane 1), which was greatly diminished by IPS-1 depletion (upper panel, lane 4). These data implied that IPS-1 might be essential for the dsRNA-dependent dimerization of PKR, but not for the dsRNA-independent dimerization.

IPS-1 physically interacts with PKR

To determine the underlying mechanism by which IPS-1 promotes PKR activation, we tested the possibility that IPS-1 interacts with PKR. A549 cells were co-transfected with plasmids expressing IPS-1–FLAG and PKR–HA fusion proteins, and were harvested for the co-IP assay using antibodies against HA or FLAG. The results showed that the anti-HA antibody was able to co-immunoprecipitate PKR or IPS-1 when they were expressed together in the absence or presence of poly(I:C) (Fig. 4A). Similarly, anti-FLAG antibody co-immunoprecipitated both PKR and IPS-1 in the mock- or poly(I:C)-transfected cells (Fig. 4A). To validate the interaction between IPS-1 and PKR, purified IPS-1–FLAG and PKR–HA were incubated *in vitro*, followed by a pulldown assay using antibodies against FLAG or HA. Our data revealed that the anti-FLAG antibody was able to pull down both IPS-1–FLAG and the PKR–HA (Fig. 4B). Reciprocally, the anti-HA antibody also pulled down both proteins (Fig. 4C). Next, IPS-1–His or PKR–GST fusion proteins were expressed in *Escherichia coli* and purified by using antibodies against GST or His respectively. IPS-1–His and PKR–GST were

Journal of Cell Science (2014) 127, 2471–2482 doi:10.1242/jcs.139626

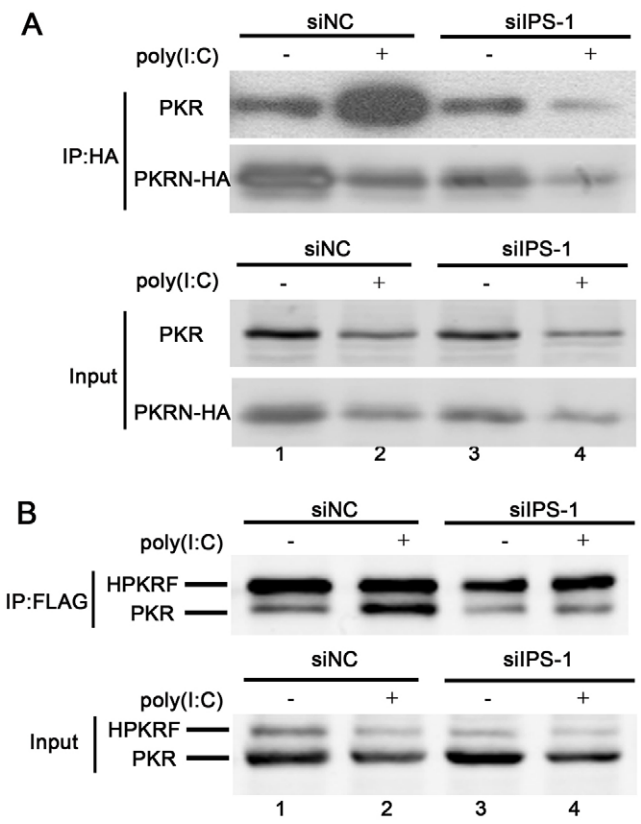

Fig. 3. IPS-1 mediates the association of endogenous PKR with its dsRBDs or with exogenously expressed full-length PKR. A549 cells were transfected with siNC or siIPS-1, together with plasmids expressing PKRN–HA (A) or HPKRF (B), followed by poly(I:C) transfection. Immunoprecipitations (IP) were performed using anti-HA or anti-FLAG antibody. Protein complexes were separated by SDS-PAGE and detected by western blotting using the anti-PKR antibody. Data are representative of at least three independent experiments.

incubated *in vitro*, followed by a pulldown assay using GST resin. The western blot clearly showed that IPS-1 was co-precipitated with PKR in the absence or presence of poly(I:C) (Fig. 4D). These co-IP and GST pulldown data indicate that IPS-1 has a direct interaction with PKR that is independent of dsRNA.

The dsRBDs of PKR and CARD of IPS-1 mediate the IPS-1-PKR interaction

To map which domains of PKR and IPS-1 are responsible for their interaction, we generated a series of constructs expressing different forms of PKR or IPS-1. The PKR protein forms included full-length PKR (PKR–HA), the N-terminus of PKR comprising two dsRNA binding domains (dsRBDs) (PKRN–HA) and the C-terminus of PKR comprising the kinase domain (PKRC–HA) (Fig. 5A). The IPS-1 protein forms included full-length IPS-1 (IPS-1–FLAG), IPS-1 with CARD deleted (ΔCARD–FLAG), IPS-1 with deletion of the proline-rich domain (ΔPro–FLAG) and IPS-1 with deletion of the transmembrane domain (ΔTM–FLAG) (Fig. 5B). Cells were transfected with the plasmid encoding IPS-1–FLAG, along with the plasmid encoding PKR–HA, PKRN–HA or PKRC–HA, followed by co-IP assay using anti-FLAG antibody. The western blotting data showed that the anti-FLAG antibody immunoprecipitated IPS-1–FLAG with PKR–HA or PKRN–HA but not with PKRC–HA, indicating that the dsRBDs of PKR mediate its association with IPS-1 (Fig. 5C). Subsequently, cells were transfected with PKR–HA-expressing plasmid, along with the plasmid encoding IPS-1–FLAG, ΔCARD–FLAG, ΔPro–FLAG or ΔTM–FLAG, followed by co-IP assay using an anti-FLAG antibody. PKR was immunoprecipitated with IPS-1–FLAG, ΔPro–FLAG or ΔTM–FLAG but not with ΔCARD–FLAG (Fig. 5D). Furthermore, an *in vitro* PKR kinase assay was performed using purified full-length and deletion forms of IPS-1. Western blotting using an antibody that detected p-PKR (Thr446) showed that the presence of IPS-1–FLAG, ΔPro–FLAG or ΔTM–FLAG clearly increased PKR phosphorylation at Thr446, whereas ΔCARD–FLAG only weakly promoted PKR activation (Fig. 5E). These data suggested that CARD is indispensable for mediating the IPS-1–PKR interaction and PKR activation.

PKR is translocated into stress granules upon stimulation with dsRNA

As PKR has been reported to be a component of stress granules that are induced by several viruses (Okonski and Samuel, 2013; Onomoto et al., 2012), we next used immunofluorescence microscopy to examine whether PKR is recruited to stress granules upon stimulation of cells with dsRNA. In A549 and HeLa cells, PKR was diffusely distributed in the cytoplasm, whereas TIA-1 was predominantly located in the nuclei. In both dsRNA-stimulated A549 and HeLa cells, nuclear TIA-1 translocated to cytoplasmic granules as expected. Interestingly, PKR protein was localized in the granules that overlapped with regions of TIA-1 staining (Fig. 6A,B), suggesting that PKR was recruited by dsRNA-induced stress granules. As the compositions of stress granules vary in response to different stresses (Kedersha et al., 2005), we also examined whether PKR is a component of stress granules that are induced by other stresses. After heat shock or hippuristanol treatment, A549 and HeLa cells were stained with antibodies against PKR and TIA-1. In response to heat shock or hippuristanol, TIA-1 translocated from nuclei to form cytoplasmic stress granules (Fig. 6A,B), in agreement with previous reports (Anderson and Kedersha, 2008; Gilks et al., 2004). By contrast, PKR remained evenly distributed in the cytoplasm after heat shock or hippuristanol stimulation (Fig. 6A,B). The colocalization analysis showed that the overlap coefficient between PKR and TIA-1 was significantly higher in dsRNA-stimulated cells, but not in heat-shock- or hippuristanol-stressed cells, than in the mock-treated cells (0.86 versus 0.53 in A549, $P<0.01$, Fig. 6C; 0.8 versus 0.56 in HeLa, $P<0.01$, Fig. 6D), indicating that the recruitment of PKR to stress granules is stress specific.

IPS-1 formed non-stress-granule clusters on mitochondrial membranes upon dsRNA stimulation

To test whether IPS-1 is recruited to stress granules together with PKR, IPS-1 subcellular localization was visualized by confocal immunofluorescence staining microscopy using a mitochondrial indicator, MitoTracker Red, and antibodies against IPS-1 and TIA-1. The staining pattern of IPS-1 overlapped with that of MitoTracker Red in control cells, whereas, in dsRNA-stimulated cells, IPS-1 protein formed clusters that partially overlapped with MitoTracker Red (Fig. 7A). In addition, cells were double-stained with antibodies against TIA-1 and IPS-1 (Fig. 7B), or TIA-1 antibody and MitoTracker Red (Fig. 7C). A small amount of TIA-1 aggregates were observed to overlap with IPS-1-positive clusters, whereas TIA-1-positive stress granules did not colocalize with MitoTracker Red. The colocalization analysis

Journal of Cell Science (2014) 127, 2471–2482 doi:10.1242/jcs.139626

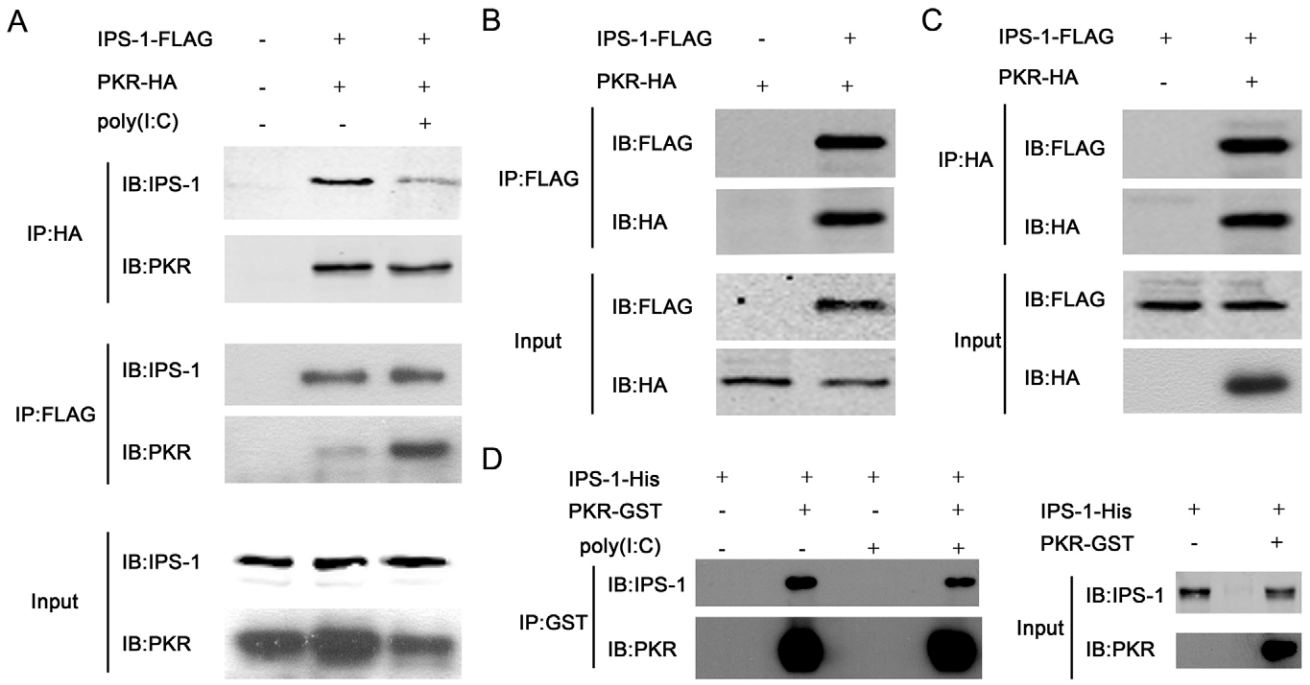

Fig. 4. IPS-1 physically associates with PKR. (A) Co-IP assay. A549 cells were co-transfected with plasmids expressing IPS-1–FLAG and PKR–HA, followed by mock or poly(I:C) stimulation. Whole-cell extracts were prepared for immunoprecipitations (IP) using antibody against HA or FLAG respectively. (B,C) Pulldown assay. Purified IPS-1–FLAG and PKR–HA proteins were incubated with FLAG or HA antibodies. (D) Pulldown assay. IPS-1–His and PKR–GST fusion proteins purified from *E. coli* were incubated in the absence or presence of poly(I:C) and then pulled down with GST resin. Protein complexes were separated by SDS-PAGE and detected by western blotting (IB) with antibodies against the indicated proteins. Data are representative of at least three independent experiments.

revealed that the overlap coefficient between TIA-1 and IPS-1 was slightly, but not significantly, increased in poly(I:C)-treated cells ($P>0.05$, Fig. 7D), and the overlap coefficients between TIA-1 and MitoTracker Red were comparable in mock and poly(I:C)-treated cells (Fig. 7D).

The formation of stress granules and innate immune responses induced by dsRNA show anti-VSV activities

To determine whether stress granules or innate immune responses play a role in cell physiology or viral replication, we infected the cells with vesicular stomatitis virus carrying the gene encoding GFP (VSV-GFP). As IPS-1 and PKR function in both signaling pathways, we silenced two additional proteins – RIG-I, the receptor sensing VSV, and G3BP-1, a key component of stress granules. As predicted, the depletion of RIG-I, IPS-1 and PKR significantly decreased the level of dsRNA-induced IFN-β expression (Fig. 8A). Although G3BP-1 knockdown largely abolished the stress granule formation induced by dsRNA (data not shown), its depletion barely affected the induction of IFN-β. Moreover, the cell viabilities were comparable among all the mock-treated cells (around 85%, Fig. 8B) or among the dsRNA-treated cells (around 75%, Fig. 8B), suggesting that either stress granule formation or innate immune response do not have a pronounced effect on cell survival upon VSV infection. In the mock-treated cells, the percentages of VSV-GFP-positive cells were comparable (approximately 75%) in most tested cells except those with RIG-I knockdown, agreeing with our previous finding that PKR is not a major anti-VSV protein (Zhang and Samuel, 2007). In dsRNA-stressed cells, the percentage of cells that were positive for GFP was largely reduced in siNC-transfected cells (5.6%), as a result of IFN induction and stress granule formation induced by dsRNA. Moreover, the percentage of cells with GFP staining was significantly restored by depletion of PKR, IPS-1 or G3BP-1 (around 15.9%, 16.2% and 9.0% of cells were GFP positive, respectively, Fig. 8C,D). These data suggested that stress granules and innate immune responses confer an advantage in protecting cells against VSV infection. Surprisingly, RIG-I knockdown led to decreased viral replication in mock-treated cells (39% GFP-positive cells, $P<0.01$, Fig. 8C,D) and a comparable viral replication in dsRNA-stressed cells (3.8% GFP-positive cells, $P>0.05$, Fig. 8C,D), implying that RIG-I might play some proviral role in VSV replication.

DISCUSSION

Stress granule formation and innate immunity are two distinct mechanisms by which cells defend themselves from stresses derived from viral infection. Herein, we have investigated their relationship by studying the role of four innate immune proteins in the stress granule response, and our data provide several novel findings and implicate IPS-1 in the formation of stress granules.

In the present study, dsRNA was used as a major stimulator to induce stress granule formation because it is a known activator of innate immunity and represents a common stress encountered during viral infection. We demonstrated that one of the dsRNA sensors, PKR, is a dominant factor controlling eIF2α activation and the process of stress granule formation under conditions of dsRNA-induced stress, agreeing with our previous observation that PKR is the only kinase mediating dsRNA-induced phosphorylation of eIF2α (Zhang and Samuel, 2007). This observation further extends the notion that PKR plays a key role in viral-infection-induced stress granule formation, as

Journal of Cell Science (2014) 127, 2471–2482 doi:10.1242/jcs.139626

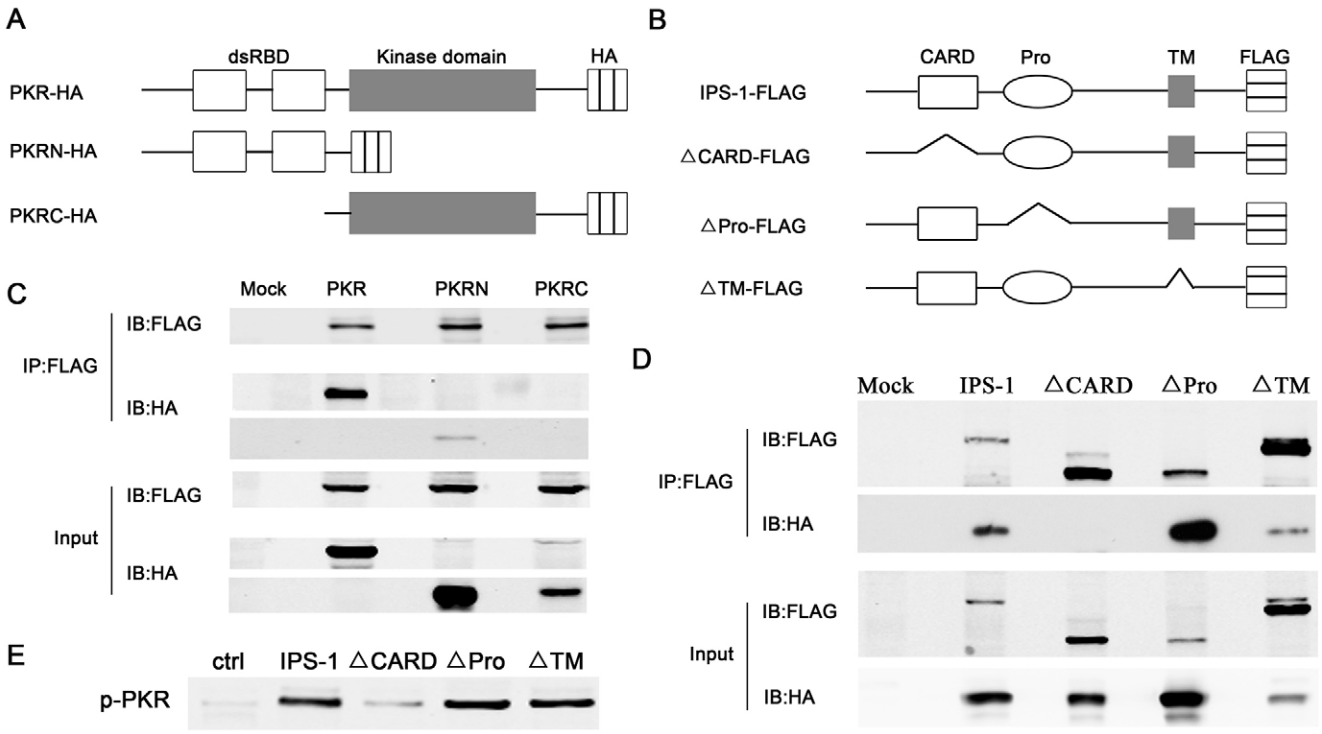

Fig. 5. The dsRBDs of PKR and CARD of IPS-1 mediate their interaction. (A,B) Schematic representation of full-length and truncated forms of PKR and IPS-1 proteins. Pro, proline domain; TM, transmembrane domain. Cells were co-transfected with plasmids expressing different forms of PKR and full-length IPS-1 (C), or were co-transfected with plasmids expressing different forms of IPS-1 and full-length PKR (D). Transfected cells were harvested for immunoprecipitation (IP) using the anti-FLAG antibody. Protein complexes were separated by SDS-PAGE and detected by western blotting (IB) with the indicated antibodies. Data are representative of at least three independent experiments. (E) PKR kinase assay. Purified PKR and full-length or deletion forms of IPS-1 were incubated in kinase reaction mixture for 30 min. Reaction mixtures were used for western blotting to detect PKR phosphorylation at Thr446. Ctrl, control.

reported for RNA viruses, including measles virus, hepatitis C virus, IAV and respiratory syncytial virus (Dabo and Meurs, 2012; Lindquist et al., 2011; Okonski and Samuel, 2013; Onomoto et al., 2012; Ruggieri et al., 2012). It is conceivable that PKR most likely is the major eIF2α kinase involved in the stress granule formation that is induced by other dsRNA-producing viruses, either DNA or RNA viruses.

Importantly, the innate immune adaptor IPS-1 was found to have a novel function in regulating stress granule formation, which is mediated through PKR. To date, IPS-1 has been implicated as a common adaptor in a variety of signaling pathways, owing to its ability to interplay with different signaling molecules. Initially, IPS-1 was identified as a common adaptor of RIG-I and MDA5 in the innate signaling pathway triggered by viral infection or dsRNA (McWhirter et al., 2005). Subsequently, IPS-1 was found to interact with a sensor of DNA and dsRNA, DHX9, in myeloid dendritic cells (Zhang et al., 2011). Most recently, IPS-1 was found to recruit the inflammasome protein NLRP3 to mitochondria (Arnaud et al., 2011). In the present study, we demonstrate that IPS-1 acts as an adaptor in stress granule formation, through an association with the key stress granule regulator, PKR. We show that the interaction between IPS-1 and PKR is mediated by the dsRBDs of PKR and the CARD of IPS-1. Interestingly, the deletion of the IPS-1 proline domain resulted in an increased interaction with PKR, implying that the proline domain might be an inhibitory domain or a conformational change might be required for IPS-1 to interact with PKR. By contrast, deletion of the transmembrane domain of IPS-1 led to a decreased interaction with PKR, suggesting that IPS-1 needs to be localized on the mitochondrial membrane for an optimal interaction.

Furthermore, our data indicated that the interaction between IPS-1 and PKR might directly affect the dsRNA-dependent dimerization of PKR. Our co-IP data showed that the endogenous PKR can associate with N-terminal dsRBDs or full-length PKR in the absence of dsRNA and IPS-1, agreeing with a previously established notion that PKR might form a weak dimer in latent cells (Langland and Jacobs, 1992; Patel et al., 1995). The IPS-1 depletion abrogated the dsRNA-mediated PKR–dsRBDs and PKR–PKR associations, suggesting that dsRNA-mediated PKR dimerization requires the participation of IPS-1. Consistently, we observed that the *in vivo* phosphorylation of PKR and eIF2α triggered by both HMW and LMW poly(I:C) was markedly reduced by IPS-1 depletion, and the presence of IPS-1 significantly increased the *in vitro* phosphorylation of PKR on Thr446, which is independent of, but enhanced by, dsRNA. Interestingly, in an *in vitro* assay, dsRNA alone did not lead to PKR phosphorylation on Thr446, although dsRNA has been shown to induce PKR phosphorylation (Li et al., 2006). This difference could be caused by different detection assays used – we used a specific antibody against phosphorylated Thr446, whereas the autoradiography protocol used in other studies enables the detection of phosphorylation of several sites, including Thr258, Ser242, Thr255 or Thr451, in addition to Thr446 (Romano et al., 1998; Taylor et al., 1996). As phosphorylation in the activation loop (Thr446 or Thr451) functions to facilitate substrate binding and catalysis (Williams, 1999), the observation that IPS-1 assists PKR autophosphorylation on Thr446 might illustrate a potential role of

Journal of Cell Science (2014) 127, 2471–2482 doi:10.1242/jcs.139626

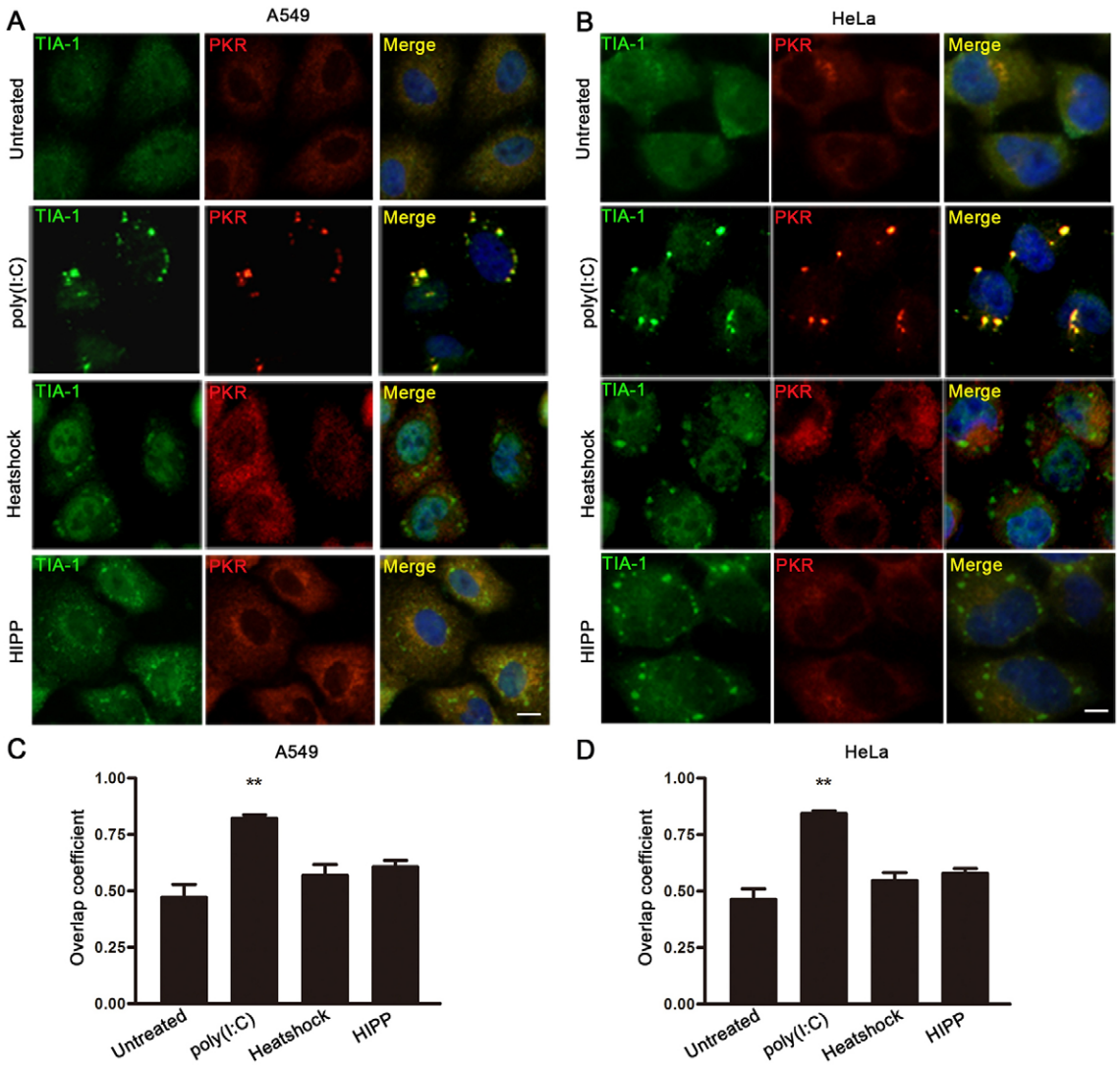

Fig. 6. PKR localizes in stress granules induced by dsRNA. A549 (A) and HeLa (B) cells were stimulated with poly(I:C), heat shock or hippuristanol (HIPP), or left untreated. Cells were processed for immunofluorescence microscopy by staining with antibodies against PKR (red) and TIA-1 (green). Nuclei were stained with DAPI (blue). Scale bars: 10 μm. (C,D) The overlap coefficient of PKR with TIA-1 was analyzed by using ZEN software for each of the two cell lines. Data are shown as the mean±s.e.m. (≥30 cells in three independent experiments were examined); ** $P<0.01$.

IPS-1 in PKR signaling. In this respect, our finding that IPS-1 interacts with PKR and facilitates its activation could help us to uncover more mechanisms of their common functions. For example, the pro-apoptotic effect of IPS-1 in response to viral infection could possibly be exerted through PKR-mediated signaling.

Our immunofluorescence studies indicated that PKR and IPS-1 might disassociate upon PKR activation. PKR protein was recruited into stress granules that were induced by dsRNA stress, but not those induced by heat shock or hippuristanol. dsRNA alone, independent of other viral gene products, is sufficient to induce the translocation of PKR into stress granules, as seen in the case of IAV-induced avSGs and measles-virus-induced stress granules (Okonski and Samuel, 2013; Onomoto et al., 2012). By contrast, IPS-1 protein forms some mitochondria-associated clusters upon dsRNA stimulation, consistent with recent reports that IPS-1 undergoes a conformational switch to produce prion-like aggregates upon viral infection or dsRNA stimulation (Hou et al., 2011; Meylan et al., 2006; Seth et al., 2005). Notably, some of these IPS-1-positive clusters overlapped with stress granules, so the possibility that IPS-1 colocalizes with stress granules could not be ruled out, as stress granule formation is a highly dynamic process.

Intriguingly, the impacts of another two dsRNA sensors, RIG-I and MDA5, on dsRNA-induced stress granule formation are distinct. RIG-I and MDA5 are responsible for recognizing different lengths of dsRNA molecules or viruses to initiate innate immune signaling (Kato et al., 2008). RIG-I was dispensable for PKR activation and stress granule formation, regardless of dsRNA lengths, which we expected as previous work has shown that the interaction between PKR and IPS-1 takes place prior to and was independent of interaction between RIG-I and IPS-1 (Arnaud et al., 2011). As for MDA5, it plays a moderate role in stress granule formation induced by HMW or LMW poly(I:C); in addition, it has a moderate effect on PKR and eIF2α phosphorylation induced by HMW dsRNA, but not by LMW dsRNA. In combination with the report that MDA is a component of stress granules (Langereis et al., 2013), and that

Journal of Cell Science (2014) 127, 2471–2482 doi:10.1242/jcs.139626

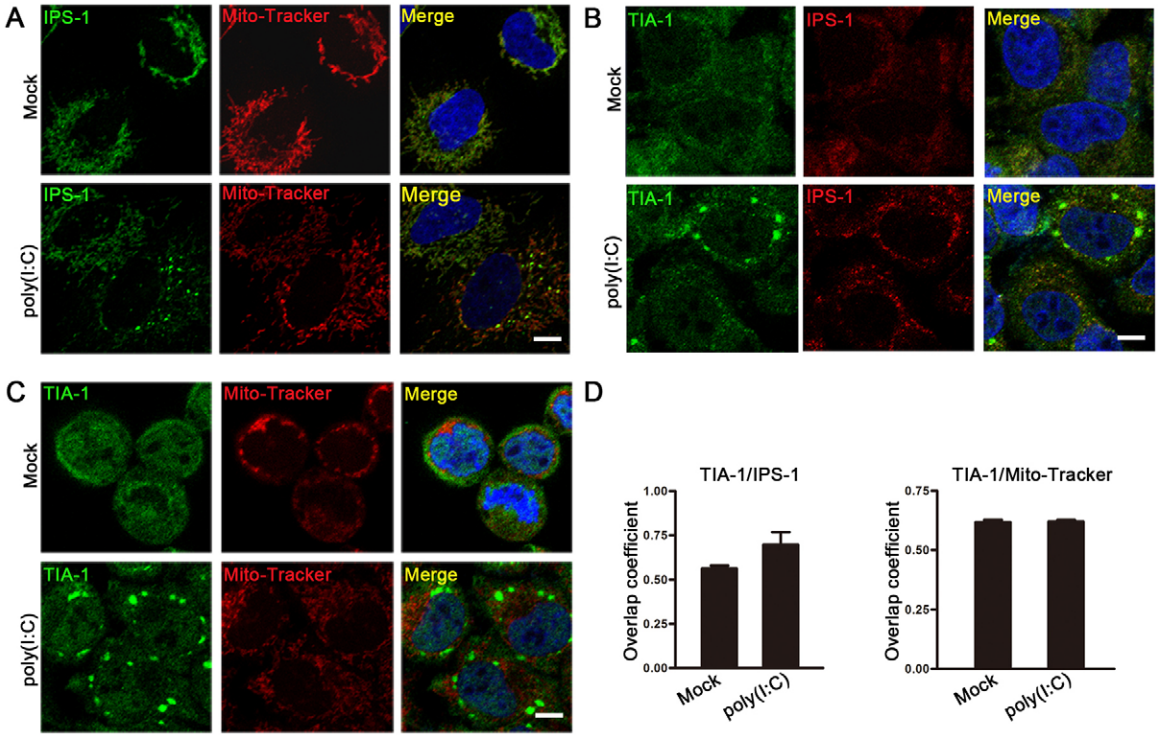

Fig. 7. IPS-1 protein forms clusters on mitochondrial membranes. A549 cells were mock-transfected or transfected with poly(I:C). Cells were incubated with MitoTracker Red and collected for confocal immunofluorescence staining microscopy. Cells were stained with antibodies against IPS-1 or TIA-1 (green), and nuclei were visualized with DAPI (blue). (A–C) Images are representative of at least three independent experiments. Scale bars: 10 μm. (D) The overlap coefficient of IPS-1 (left) or MitoTracker Red (right) with TIA-1 was analyzed by using ZEN software. Data are shown as the mean±s.e.m. (≥30 cells in three independent experiments were examined).

MDA5 displays differential effects on PKR phosphorylation and stress granule formation, we speculated that the major mechanism by which MDA5 affects stress granule formation is through mediating the assembly of stress granule components downstream of eIF2α phosphorylation, rather than through directly regulating the activation of PKR or eIF2α.

Based on the data presented here, we propose that the role of IPS-1 in PKR activation is to provide a physical platform for PKR to form dsRNA-dependent dimers. In unstressed cells, PKR protein resides in the cytoplasm as monomer or weak dimer, and dynamically interacts with IPS-1. After binding to dsRNA, PKR molecules form more dimers in association with IPS-1, thereby undergoing autophosphorylation. Activated PKR is released from IPS-1 and phosphorylates downstream eIF2α, resulting in inhibition of translation. Finally, a variety of components, including PKR, stalled initiated translation complexes and TIA-1, etc., assemble to form stress granules. After dissociation from the PKR dimer, IPS-1 interacts with RIG-I and becomes activated, forming prion-like aggregates on mitochondrial membranes (Hou et al., 2011).

We found that both stress granules and innate immunity protect cells from viral infection. Depletion of IPS-1 or PKR abolished both IFN production and stress granule formation, leading to a higher rate of VSV replication than depletion of G3BP-1 alone, which only eliminated the stress granule formation. These data suggest that innate immunity and the formation of stress granules might act cooperatively to combat VSV. In addition, as mitochondrial IPS-1 has been suggested to participate in the apoptosis induced by VSV infection (Guan et al., 2013), blockade of apoptosis by IPS-1 knockdown might be another contributing factor to the recovery of viral replication. Unexpectedly, the cell viabilities in response to VSV infection were not correspondingly decreased by depletion of IPS-1, PKR or G3BP-1, suggesting that other responses, rather than stress granule formation and innate immunity, play a dominant role in cell death caused by VSV infection.

The fact that IPS-1 and PKR participate in stress granule formation and innate signaling indicates that these two distinct responses have a close connection. To overcome stress-granule-dependent and innate immunity defenses, viruses must have developed their own strategies to counteract IPS-1 or PKR (Lifland et al., 2012; Onomoto et al., 2012; Ruggieri et al., 2012; Tu et al., 2012). However, the storage of cellular components in stress granules could potentially pose a negative effect on the innate immune response, because stress granules not only recruit innate immune signaling molecules, including PKR, RIG-I and MDA5, but also effector molecules, such as OAS, RNase L and ADAR1 (Onomoto et al., 2012; Weissbach and Scadden, 2012). Our data show that blockade of stress granule formation by G3BP-1 knockdown did not have a significant effect on dsRNA-induced IFNs, consistent with a recent study showing that the recruitment of MDA5 by stress granules did not affect the induction of type-I IFNs resulting from mengovirus infection (Langereis et al., 2013). These observations suggest that the processes of stress granule formation and innate immune signaling do not engage in direct competition for these cellular components. Nonetheless, this observation needs to be further validated in other models, because the abundances of the relevant proteins in different cells might vary.

Journal of Cell Science (2014) 127, 2471–2482 doi:10.1242/jcs.139626

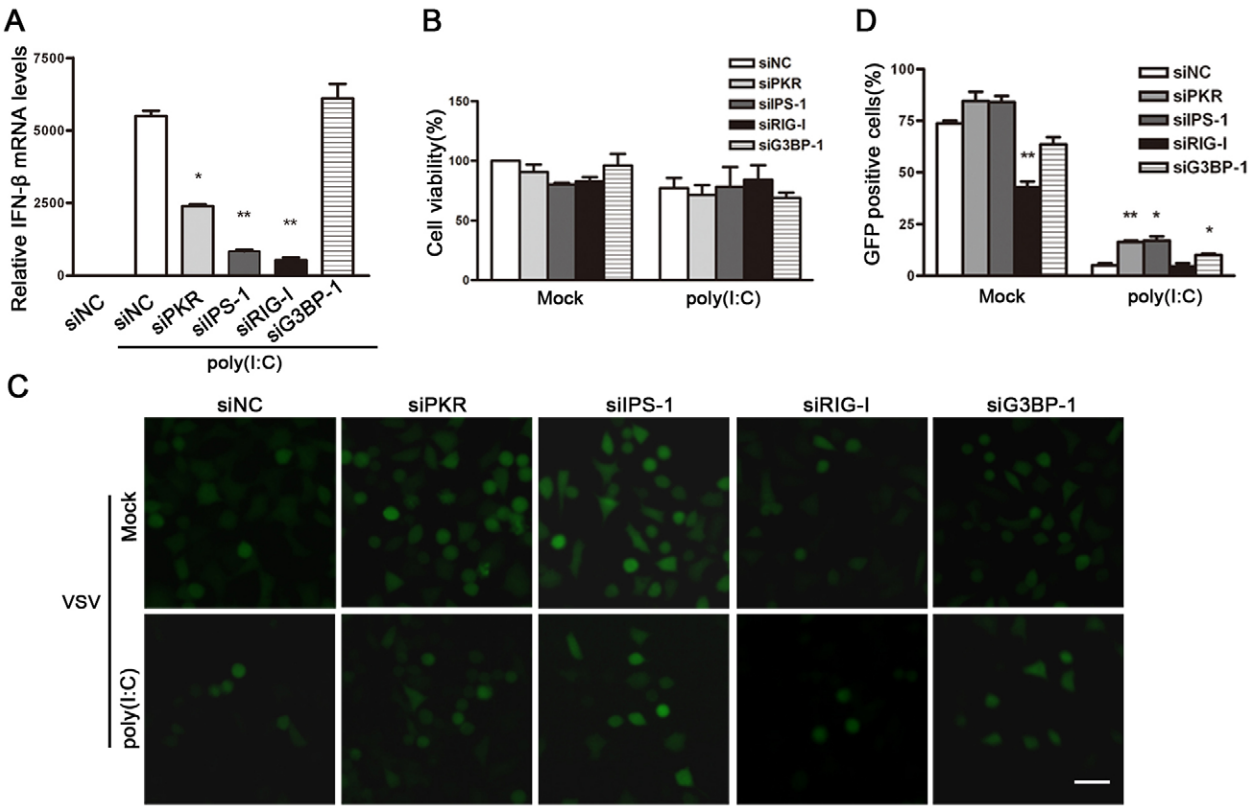

Fig. 8. Blocking innate immune signaling or stress granule formation rescues VSV-GFP replication. A549 cells were transfected with siNC, siPKR, siIPS-1, siRIG-I or siG3BP-1. At 48 h, cells were stimulated with poly(I:C) for 3 h, followed by VSV-GFP infection. (A) Total RNAs were harvested at 3 h post-poly(I:C)-transfection, and IFN-β mRNA levels were measured by real-time PCR. (B) Cell viabilities at 10 h post-infection were determined by using the MTT assay. (C) Cell images were taken at 8 h post-infection and representative images are shown. Scale bar, 10 μm. (D) PicCnt 100× was used to determine the percentages of GFP-positive cells. Data are shown as the mean±s.e.m. (≥100 cells from each culture in three independent experiments were examined);*$P<0.05$, **$P<0.01$.

In summary, our work demonstrates for the first time that IPS-1 is involved in the process of stress granule formation through its interaction with PKR, providing evidence that IPS-1 acts as a novel adaptor in an additional anti-stress response. Further investigations into the biological significance of the interaction between IPS-1 and PKR will provide us with more in-depth knowledge of the roles of IPS-1 and PKR in these cellular signaling pathways.

MATERIALS AND METHODS

Cell culture

Human lung carcinoma epithelial cells (A549), human cervical cancer cells (HeLa) and human embryonic kidney cells (293T) were maintained in Dulbecco's modified Eagle's medium (DMEM) supplemented with 5% (v/v) fetal bovine serum (Gibco, CA), 1% sodium pyruvate, 100 μg/ml penicillin and 100 units/ml streptomycin (Invitrogen, CA) at 37℃.

Stress treatments and indirect immunofluorescence staining

Cells (3×10^4) were seeded onto coverslips in 24-well plates. Cells were transfected with 300 ng of poly(I:C) (tlrl-pic, tlrl-picw, InvivoGen, MO) by using Lipofectamine 2000 (Invitrogen, CA), or were incubated at 43℃ for 1 h or incubated with 1 μM hippuristanol [kindly provided by Junichi Tanaka (Mazroui et al., 2006)] for 1 h. Cells were incubated with 50 nM MitoTracker Red (Molecular Probes) for 20 min, washed in phosphate-buffered saline (PBS) and fixed in 4% (v/v) paraformaldehyde. Cells were permeabilized in 0.2% Triton X-100 for 15 min and blocked in blocking buffer (5% bovine serum albumin in PBS) for 1 h, followed by incubation with primary antibodies and secondary antibodies. The primary antibodies used were against TIA-1 (Santa Cruz, CA), PKR (Santa Cruz, CA) and IPS-1 (BETHYL, TX). The secondary antibodies used were Cy3-conjugated goat anti-rabbit-IgG (Millipore, MA) and Alexa-Fluor-488-conjugated anti-goat-IgG (R&D, MN). Cells were then stained with 0.2 mg/ml DAPI (Invitrogen, CA) and visualized using a Zeiss fluorescence microscope or a Zeiss LSM710 confocal microscope. Positively stained cells were quantified using the PicCnt 100× software. For colocalization assays, images were typically acquired with the same optical slice thickness in every channel and analyzed by using the Carl Zeiss software ZEN. Mander's coefficient was used to measure colocalization.

Plasmids

The sequences of primers used in PCR to amplify tagged full-length PKR, IPS-1, truncated fragments of PKR and IPS-1, or PKR and IPS-1 are listed in supplementary material Table S1. The PCR templates were plasmid pEF-BOS IPS-1-FLAG (Addgene, MA) and pSG5-PKR^{RSC} (a kind gift from Stefan Rothenburg, NIH, MD) (Zhang et al., 2009). PCR fragments were cloned into the pSG5 vector for eukaryotic expression, or cloned into the pGEX-6P-1 (PKR) or pET28a (IPS-1) vector for prokaryotic expression after digestion by restriction enzymes.

RNAi

The sequences of siRNAs prepared by Invitrogen with dTdT overhangs were as follows: 5′-CCUCAUCUCUUUGUUCUAA-3′ and 5′-GCAU-GGGCCAGAAGGAUUUCA-3′ for PKR (siPKR), 5′-GGAAGAGGUG-CAGUAUAUU-3′ for RIG-I (siRIG-I), 5′-GGUGAAGGAGCAGAUU-CAG-3′ for MDA5 (siMDA5), 5′-UAGUUGAUCUCGCGGACGA-3′

and 5′-CCACCUUGAUGCCUGUGAA-3′ for IPS-1 (siIPS-1) and 5′-GAGCCAGUAUUAGAAGAAA-3′ for G3BP-1 (siG3BP-1). Dharmacon's negative siRNA with a scrambled sequence were used as a negative control (siNC). siRNAs were transfected into A549 cells by using Lipofectamine 2000 (Invitrogen, CA) according to the manufacturer's instructions.

Real-time PCR

Total RNA was prepared from A549 cells using TRIzol reagent (Invitrogen, CA) following the manufacturer's instructions. Then, 1 µg of total RNA was reverse-transcribed to produce cDNAs and then amplified using SYBR Green Master Mix (Bio-Rad, CA) following the manufacturer's protocol. The primer pairs used were as follows: glyceraldehyde-3-phosphate dehydrogenase (GAPDH), forward primer 5′-GCCTTCCGTGTCCCCACTG-3′ and reverse primer 5′-CGCCTGCTTCACCACCTTC-3′; MDA5, forward primer 5′-TGGACATAACAGCAACATGG-3′ and reverse primer 5′-CACTCTGGTTTTTCCACTCC-3′; IFN-β, forward primer 5′-AAACTCATGAGCAGTCTGCA-3′ and reverse primer 5′-AGGAGATCTTCAGTTTCGGAGG-3′. Quantitative real-time PCR was performed using the CFX96 Real-Time PCR System (Bio-Rad, CA). Relative mRNA levels were calculated after normalization to GAPDH.

Western blotting

A549 cells were seeded in 12-well plates (8×10^4 per well). After transfection with siRNAs for 48 h, cells were transfected with 1 µg poly(I:C) by using Lipofectamine 2000 (Invitrogen, CA) for 6 h. Whole-cell extracts were prepared in the presence of 1 mM phenylmethylsulfonyl fluoride (PMSF) and 1% (v/v) protease inhibitor cocktail (Sigma, MO) as described previously (Li et al., 2013). Proteins were fractionated by electrophoresis on sodium dodecyl sulphate–10% polyacrylamide gels, transferred to nitrocellulose membranes, blocked and then probed with an appropriate dilution of primary antibody in PBS containing 3% (w/v) skimmed milk. Rabbit polyclonal antibodies were used to detect PKR (Santa Cruz, CA), phospho-PKR (Epitomics, CA), phospho-eIF2α (Cell Signaling Technology, MA), RIG-I (Cell Signaling Technology, MA), IPS-1 (Bethyl, TX), HA (Sigma, MO) and FLAG (Beverly, MA); goat polyclonal antibody was used to detect eIF2α (Santa Cruz, CA), mouse monoclonal antibody was used to detect β-actin (Sigma, MO). Western blot visualization was performed with IRDye-800-CW-conjugated anti-rabbit-IgG or IRDye-680-CW-conjugated anti-mouse-IgG secondary antibodies according to the manufacturer's protocols (LI-COR, NE). Immunoreactive bands were visualized using an Odyssey infrared imaging system.

Co-immunoprecipitation assay

For the analysis of interactions between endogenous PKR and exogenously expressed PKRN–HA or full-length PKR, HeLa cells were transfected with siNC or siIPS-1 and pSG5-PKRN-HA or pSG5-HPKRF for 48 h. For analysis of the interaction between PKR and IPS-1, A549 cells (7×10^5 per well, six-well plate) were transfected with plasmids expressing IPS-1–FLAG and PKR–HA fusion proteins. Cells were then transfected with 3 µg of poly(I:C) for 1 h and collected in RIPA lysis buffer (50 mM Tris-HCl, 0.5% NP-40, 1% Triton X-100, 1 mM EDTA, 150 mM NaCl, 1 mM PMSF and 1% v/v protease inhibitor cocktail). The protein concentration was determined by using the Bradford assay. Subsequently, 1 mg of cell lysate was incubated with 20 µl of monoclonal anti-HA or anti-FLAG agarose (Sigma, MO) at 4℃ overnight. Beads were collected by centrifugation and washed extensively with NET-RIPA wash buffer (50 mM Tris-HCl, 0.5% NP-40, 1 mM EDTA, 150 mM NaCl), and proteins were eluted in SDS loading buffer.

Protein expression and purification

pSG5-IPS-1-FLAG and pSG5-PKR-HA were expressed in HEK293T cells by transient transfection. At 48 h after transfection, cells were lysed in RIPA lysis buffer and centrifuged at 12,000 ***g*** for 15 min. The supernatants were incubated with anti-FLAG or anti-HA beads (Sigma, MO) and eluted with the FLAG peptide or HA peptide (Sigma, MO). pET28A-IPS-1 and pGEX-6P-PKR were transformed into Rosetta 2(DE3). Expression of IPS-1–His and PKR–GST fusion proteins was induced by the addition of 500 µM isopropyl-β-d-thiogalactopyranoside (IPTG) at 20℃ for 16 h, and purified using His-(Merck, NJ) and GST-binding resin (Merck, NJ) according to the manufacturer's instructions.

In vitro pulldown assay

Purified full-length or truncated IPS-1 proteins were individually incubated with full-length or truncated PKR proteins for 1 h, followed by incubation with anti-FLAG or anti-HA beads for 1 h. 100 nM IPS-1–His and PKR–GST fusion proteins purified from *E. coli* were incubated in the absence or presence of 5 µg/ml poly(I:C), followed by overnight incubation with GST-binding resin. The beads were collected by centrifugation and proteins were eluted in SDS loading buffer for western blot analysis.

PKR activation assay

Autophosphorylation assay of PKR was performed in kinase buffer (20 mM Tris-HCl pH 7.6, 50 mM KCl, 25 mM $MgCl_2$, 1% protease inhibitor cocktail and 1 mM PMSF) containing purified PKR, full-length or deletion forms of IPS-1, dsRNA (2 mg/ml) and ATP (0.1 mM) at 30℃ for 30 min. Reaction mixtures were analyzed by SDS-PAGE and western blotting using the anti-phospho-PKR antibody (Thr 446) (Epitomics, CA).

Viral infection

Vesicular stomatitis virus (VSV-GFP) was kindly provided by Dongyan Jin (Kok et al., 2011). A549 cells were transfected with siRNAs against PKR, IPS-1, RIG-I or G3BP-1 for 48 h. Cells was transfected with poly(I:C) for 3 h and then infected with VSV-GFP (multiplicity of infection=1). Total cellular RNAs were extracted before viral infection and analyzed by real-time PCR to determine the IFN-β mRNA levels. Cell viability was assessed by using the MTT [3-(4,5-dimethylthiazol-2-yl)-2,5-diphenyl-2H tetrazolium bromide] assay. Fluorescence microscopy images were taken at 8-h post-infection to visualize the viral replication.

Statistical analysis

Statistical significance was determined by using unpaired two-tailed Student's *t*-tests. $P<0.05$ was considered to be statistically significant.

Acknowledgements

We thank Junichi Tanaka (University of the Ryukyus, Okinawa, Japan) for generously providing hippuristanol, and we thank Dongyan Jin (University of Hong Kong, Pokfulam, Hong Kong) for generously providing VSV–GFP. We thank Chia-Yi Yu (National Defense Medical Center, Taipei, Taiwan.) and Yi-Ling Lin (National Defense Medical Center, Taipei, Taiwan.) for their helpful suggestion on IPS-1 expression, and we thank Meili Wei (Sun Yat-sen University, GuangZhou, China.) for assistance on IPS-1 purification.

Competing interests

The authors declare no competing interests.

Author contributions

Ping Zhang, Peifen Zhang, Y.L. and X.H. conceived and designed the experiments; experiments were carried out by Peifen Zhang, Y.L., J.X., J.H., J.P., J.X., L.F.; The data was analyzed by Peifen Zhang, Y.L. and Ping Zhang; the manuscript was written by Ping Zhang and Peifen Zhang. All authors read and approved the manuscript.

Funding

This work was supported by National Natural Science Foundation of China [grant numbers 81171576, 81371794 and 81261160323]; Guangdong Natural Science Foundation [grant number S2013010016454]; National Basic Research Program of China [grant number 2010CB530004]; Guangdong Province Universities and Colleges Pearl River School Funded Scheme [grant number 2009]; Guangdong Innovative Research Team Program [grant number 2009010058]; and Fundamental Research Funds for the Central Universities.

Supplementary material

Supplementary material available online at
http://jcs.biologists.org/lookup/suppl/doi:10.1242/jcs.139626/-/DC1

References

Akira, S. and Takeda, K. (2004). Toll-like receptor signalling. *Nat. Rev. Immunol.* **4**, 499-511.

Alexopoulou, L., Holt, A. C., Medzhitov, R. and Flavell, R. A. (2001). Recognition of double-stranded RNA and activation of NF-kappaB by Toll-like receptor 3. *Nature* **413**, 732-738.

Anderson, P. and Kedersha, N. (2002). Visibly stressed: the role of eIF2, TIA-1, and stress granules in protein translation. *Cell Stress Chaperones* **7**, 213-221.

Anderson, P. and Kedersha, N. (2008). Stress granules: the Tao of RNA triage. *Trends Biochem. Sci.* **33**, 141-150.

Arimoto, K., Fukuda, H., Imajoh-Ohmi, S., Saito, H. and Takekawa, M. (2008). Formation of stress granules inhibits apoptosis by suppressing stress-responsive MAPK pathways. *Nat. Cell Biol.* **10**, 1324-1332.

Arnaud, N., Dabo, S., Akazawa, D., Fukasawa, M., Shinkai-Ouchi, F., Hugon, J., Wakita, T. and Meurs, E. F. (2011). Hepatitis C virus reveals a novel early control in acute immune response. *PLoS Pathog.* **7**, e1002289.

Dabo, S. and Meurs, E. F. (2012). dsRNA-dependent protein kinase PKR and its role in stress, signaling and HCV infection. *Viruses* **4**, 2598-2635.

Gilks, N., Kedersha, N., Ayodele, M., Shen, L., Stoecklin, G., Dember, L. M. and Anderson, P. (2004). Stress granule assembly is mediated by prion-like aggregation of TIA-1. *Mol. Biol. Cell* **15**, 5383-5398.

Grousl, T., Ivanov, P., Malcova, I., Pompach, P., Frydlova, I., Slaba, R., Senohrabkova, L., Novakova, L. and Hasek, J. (2013). Heat shock-induced accumulation of translation elongation and termination factors precedes assembly of stress granules in S. cerevisiae. *PLoS ONE* **8**, e57083.

Guan, K., Zheng, Z., Song, T., He, X., Xu, C., Zhang, Y., Ma, S., Wang, Y., Xu, Q., Cao, Y. et al. (2013). MAVS regulates apoptotic cell death by decreasing K48-linked ubiquitination of voltage-dependent anion channel 1. *Mol. Cell. Biol.* **33**, 3137-3149.

Hou, F., Sun, L., Zheng, H., Skaug, B., Jiang, Q. X. and Chen, Z. J. (2011). MAVS forms functional prion-like aggregates to activate and propagate antiviral innate immune response. *Cell* **146**, 448-461.

Kang, D. C., Gopalkrishnan, R. V., Wu, Q., Jankowsky, E., Pyle, A. M. and Fisher, P. B. (2002). mda-5: An interferon-inducible putative RNA helicase with double-stranded RNA-dependent ATPase activity and melanoma growth-suppressive properties. *Proc. Natl. Acad. Sci. USA* **99**, 637-642.

Kato, H., Takeuchi, O., Mikamo-Satoh, E., Hirai, R., Kawai, T., Matsushita, K., Hiiragi, A., Dermody, T. S., Fujita, T. and Akira, S. (2008). Length-dependent recognition of double-stranded ribonucleic acids by retinoic acid-inducible gene-I and melanoma differentiation-associated gene 5. *J. Exp. Med.* **205**, 1601-1610.

Kawai, T., Takahashi, K., Sato, S., Coban, C., Kumar, H., Kato, H., Ishii, K. J., Takeuchi, O. and Akira, S. (2005). IPS-1, an adaptor triggering RIG-I- and Mda5-mediated type I interferon induction. *Nat. Immunol.* **6**, 981-988.

Kedersha, N. and Anderson, P. (2002). Stress granules: sites of mRNA triage that regulate mRNA stability and translatability. *Biochem. Soc. Trans.* **30**, 963-969.

Kedersha, N., Stoecklin, G., Ayodele, M., Yacono, P., Lykke-Andersen, J., Fritzler, M. J., Scheuner, D., Kaufman, R. J., Golan, D. E. and Anderson, P. (2005). Stress granules and processing bodies are dynamically linked sites of mRNP remodeling. *J. Cell Biol.* **169**, 871-884.

Kim, B., Cooke, H. J. and Rhee, K. (2012). DAZL is essential for stress granule formation implicated in germ cell survival upon heat stress. *Development* **139**, 568-578.

Kok, K. H., Lui, P. Y., Ng, M. H., Siu, K. L., Au, S. W. and Jin, D. Y. (2011). The double-stranded RNA-binding protein PACT functions as a cellular activator of RIG-I to facilitate innate antiviral response. *Cell Host Microbe* **9**, 299-309.

Langereis, M. A., Feng, Q. and van Kuppeveld, F. J. (2013). MDA5 localizes to stress granules, but this localization is not required for the induction of type I interferon. *J. Virol.* **87**, 6314-6325.

Langland, J. O. and Jacobs, B. L. (1992). Cytosolic double-stranded RNA-dependent protein kinase is likely a dimer of partially phosphorylated Mr = 66,000 subunits. *J. Biol. Chem.* **267**, 10729-10736.

Lemaire, P. A., Tessmer, I., Craig, R., Erie, D. A. and Cole, J. L. (2006). Unactivated PKR exists in an open conformation capable of binding nucleotides. *Biochemistry* **45**, 9074-9084.

Li, S., Peters, G. A., Ding, K., Zhang, X., Qin, J. and Sen, G. C. (2006). Molecular basis for PKR activation by PACT or dsRNA. *Proc. Natl. Acad. Sci. USA* **103**, 10005-10010.

Li, Y., Xie, J., Wu, S., Xia, J., Zhang, P., Liu, C., Zhang, P. and Huang, X. (2013). Protein kinase regulated by dsRNA downregulates the interferon production in dengue virus- and dsRNA-stimulated human lung epithelial cells. *PLoS ONE* **8**, e55108.

Lifland, A. W., Jung, J., Alonas, E., Zurla, C., Crowe, J. E., Jr and Santangelo, P. J. (2012). Human respiratory syncytial virus nucleoprotein and inclusion bodies antagonize the innate immune response mediated by MDA5 and MAVS. *J. Virol.* **86**, 8245-8258.

Lindquist, M. E., Mainou, B. A., Dermody, T. S. and Crowe, J. E., Jr (2011). Activation of protein kinase R is required for induction of stress granules by respiratory syncytial virus but dispensable for viral replication. *Virology* **413**, 103-110.

Mazroui, R., Sukarieh, R., Bordeleau, M. E., Kaufman, R. J., Northcote, P., Tanaka, J., Gallouzi, I. and Pelletier, J. (2006). Inhibition of ribosome recruitment induces stress granule formation independently of eukaryotic initiation factor 2alpha phosphorylation. *Mol. Biol. Cell* **17**, 4212-4219.

McWhirter, S. M., Tenoever, B. R. and Maniatis, T. (2005). Connecting mitochondria and innate immunity. *Cell* **122**, 645-647.

Meylan, E., Tschopp, J. and Karin, M. (2006). Intracellular pattern recognition receptors in the host response. *Nature* **442**, 39-44.

Ohn, T. and Anderson, P. (2010). The role of posttranslational modifications in the assembly of stress granules. *Wiley Interdiscip Rev. RNA* **1**, 486-493.

Okonski, K. M. and Samuel, C. E. (2013). Stress granule formation induced by measles virus is protein kinase PKR dependent and impaired by RNA adenosine deaminase ADAR1. *J. Virol.* **87**, 756-766.

Onomoto, K., Jogi, M., Yoo, J. S., Narita, R., Morimoto, S., Takemura, A., Sambhara, S., Kawaguchi, A., Osari, S., Nagata, K. et al. (2012). Critical role of an antiviral stress granule containing RIG-I and PKR in viral detection and innate immunity. *PLoS ONE* **7**, e43031.

Patel, R. C. and Sen, G. C. (1998). Requirement of PKR dimerization mediated by specific hydrophobic residues for its activation by double-stranded RNA and its antigrowth effects in yeast. *Mol. Cell. Biol.* **18**, 7009-7019.

Patel, R. C., Stanton, P., McMillan, N. M., Williams, B. R. and Sen, G. C. (1995). The interferon-inducible double-stranded RNA-activated protein kinase self-associates in vitro and in vivo. *Proc. Natl. Acad. Sci. USA* **92**, 8283-8287.

Qin, Q., Carroll, K., Hastings, C. and Miller, C. L. (2011). Mammalian orthoreovirus escape from host translational shutoff correlates with stress granule disruption and is independent of eIF2alpha phosphorylation and PKR. *J. Virol.* **85**, 8798-8810.

Romano, P. R., Garcia-Barrio, M. T., Zhang, X., Wang, Q., Taylor, D. R., Zhang, F., Herring, C., Mathews, M. B., Qin, J. and Hinnebusch, A. G. (1998). Autophosphorylation in the activation loop is required for full kinase activity in vivo of human and yeast eukaryotic initiation factor 2alpha kinases PKR and GCN2. *Mol. Cell. Biol.* **18**, 2282-2297.

Ruggieri, A., Dazert, E., Metz, P., Hofmann, S., Bergeest, J. P., Mazur, J., Bankhead, P., Hiet, M. S., Kallis, S., Alvisi, G. et al. (2012). Dynamic oscillation of translation and stress granule formation mark the cellular response to virus infection. *Cell Host Microbe* **12**, 71-85.

Sadler, A. J. (2010). Orchestration of the activation of protein kinase R by the RNA-binding motif. *J. Interferon Cytokine Res.* **30**, 195-204.

Saelens, X., Kalai, M. and Vandenabeele, P. (2001). Translation inhibition in apoptosis: caspase-dependent PKR activation and eIF2-alpha phosphorylation. *J. Biol. Chem.* **276**, 41620-41628.

Seth, R. B., Sun, L., Ea, C. K. and Chen, Z. J. (2005). Identification and characterization of MAVS, a mitochondrial antiviral signaling protein that activates NF-kappaB and IRF 3. *Cell* **122**, 669-682.

Takeuchi, O. and Akira, S. (2010). Pattern recognition receptors and inflammation. *Cell* **140**, 805-820.

Taylor, D. R., Lee, S. B., Romano, P. R., Marshak, D. R., Hinnebusch, A. G., Esteban, M. and Mathews, M. B. (1996). Autophosphorylation sites participate in the activation of the double-stranded-RNA-activated protein kinase PKR. *Mol. Cell. Biol.* **16**, 6295-6302.

Tsai, N. P. and Wei, L. N. (2010). RhoA/ROCK1 signaling regulates stress granule formation and apoptosis. *Cell. Signal.* **22**, 668-675.

Tu, Y. C., Yu, C. Y., Liang, J. J., Lin, E., Liao, C. L. and Lin, Y. L. (2012). Blocking double-stranded RNA-activated protein kinase PKR by Japanese encephalitis virus nonstructural protein 2A. *J. Virol.* **86**, 10347-10358.

Wehner, K. A., Schütz, S. and Sarnow, P. (2010). OGFOD1, a novel modulator of eukaryotic translation initiation factor 2alpha phosphorylation and the cellular response to stress. *Mol. Cell. Biol.* **30**, 2006-2016.

Weissbach, R. and Scadden, A. D. (2012). Tudor-SN and ADAR1 are components of cytoplasmic stress granules. *RNA* **18**, 462-471.

Williams, B. R. (1999). PKR; a sentinel kinase for cellular stress. *Oncogene* **18**, 6112-6120.

Yoneyama, M., Kikuchi, M., Natsukawa, T., Shinobu, N., Imaizumi, T., Miyagishi, M., Taira, K., Akira, S. and Fujita, T. (2004). The RNA helicase RIG-I has an essential function in double-stranded RNA-induced innate antiviral responses. *Nat. Immunol.* **5**, 730-737.

Zhang, P. and Samuel, C. E. (2007). Protein kinase PKR plays a stimulus- and virus-dependent role in apoptotic death and virus multiplication in human cells. *J. Virol.* **81**, 8192-8200.

Zhang, P., Langland, J. O., Jacobs, B. L. and Samuel, C. E. (2009). Protein kinase PKR-dependent activation of mitogen-activated protein kinases occurs through mitochondrial adapter IPS-1 and is antagonized by vaccinia virus E3L. *J. Virol.* **83**, 5718-5725.

Zhang, Z., Yuan, B., Lu, N., Facchinetti, V. and Liu, Y. J. (2011). DHX9 pairs with IPS-1 to sense double-stranded RNA in myeloid dendritic cells. *J. Immunol.* **187**, 4501-4508.